EPJ Web of Conferences **38**, 09003 (2012)
DOI: 10.1051/epjconf/20123809003
© Owned by the authors, published by EDP Sciences, 2012

Time-dependent Hartree-Fock studies of the dynamical fusion threshold

Lu Guo[1,2,a] and Takashi Nakatsukasa[2]

[1] College of Physical Sciences, University of Chinese Academy of Sciences, Beijing 100049, China
[2] RIKEN Nishina Center, Hirosawa, Wako-shi, Saitama 351-0198, Japan

Abstract. A microscopic description of dynamical fusion threshold in heavy ion collisions is performed in the framework of time-dependent Hartree-Fock (TDHF) theory using Skyrme energy density functional (EDF). TDHF fusion threshold is in a better agreement with experimental fusion barrier. We find that the onset of extra push lies at the effective fissility 33, which is consistent with the prediction of Swiatecki's macroscopic model. The extra push energy in our TDHF simulation is systematically smaller than the prediction in macroscopic model. The important dynamical effects and the way to fit the parameter might be responsible for the different results.

1 Introduction

With the experimental availability of radioactive ion beams, the study of heavy-ion fusion reactions is of great interest especially for the synthesis of superheavy elements and nuclei far from stability. The nuclear reactions at energies near the fusion barrier provides important information on the reaction mechanism and collision dynamics. Theoretical investigation is of fundamental importance to select the optimal combination of projectile and target as well as incident energy owing to the very time-consuming experiments.

The macroscopic models [1–7] used for the study of fusion reactions are successful in describing some aspects of reaction dynamics, however they have in common several shortcomings. First, nuclear structure and reaction dynamics are treated in the discrete theoretical frameworks. It is known that nuclear structure may strongly affect the reaction dynamics. For instance, different structure may change the production cross section of superheavy elements several orders of magnitudes. Second, important dynamical effects are not included in the time evolution. Dynamical effects, e.g., nucleon transfer and shape transition, are considered to play an important role on the reaction behavior. In many of macroscopic calculations, frozen density or sudden approximation has been used, where the nuclear density is assumed to be unchanged and equal to their ground-state density at any time. The collision system allows for the rearrangement of nuclear density, hence the dynamical rearrangement effect is neglected in the macroscopic model. Third, there are free parameters in the description of nuclear dynamics. These parameters are fitted with the experimental reaction data. The availability of experimental data and the way to fit the parameters will affect the reliability of theoretical predictions in macroscopic model. For example, the parameters for unmeasured reaction systems have not yet been determined in coupled channel model [8,9].

These shortcomings can be overcome with a fully microscopic theory, e.g., time-dependent Hartree-Fock (TDHF) theory. The main approximation of the theory is that the many-body wave functions are treated as independent particle states at each time. TDHF theory, proposed by Dirac in 1930 [10], was first applied in the studies of heavy-ion fusion reactions and giant resonances dynamics for more than 30 years ago [11]. At that time, simplified effective interaction and symmetry restrictions [12–15] have been employed to reduce the computational time. These limitations turned out to be a hindrance for the development [16]. With the upgrade of computer power, three-dimensional TDHF simulation with full Skyrme effective interaction becomes possible and revived the new interests in nuclear dynamics as seen from an impressive series of recent publications [17–35].

Dynamical fusion threshold is of a fundamental issue in fusion reactions. Extra push dynamics has been predicted in macroscopic models for heavy collision systems with critical fissility larger than 33 [36] and typical charge products of projectile and target larger than 1600 [37]. The extra push is provided by an additional bombarding energy over the barrier height in order to achieve a fused system. For light nuclei, since the Coulomb repulsive force is small compared to the nuclear force, the system will evolve automatically to a fused system at bombarding energies above the fusion barrier. When the charges of the projectile and target are increased, the repulsive potential energy of the system becomes so large that the system has to overcome, in order to achieve fusion, the saddle point associated with the fission barrier of a compound nucleus. The energy difference between fusion barrier and fission barrier is known as extra push energy. Recently, the experimental evidence [38–40] indicates that the extra push energy, needed in the formation of heavy and superheavy systems, is smaller than the prediction with macroscopic model [36].

Dynamical fusion threshold, which is a microscopic analog of the macroscopic extra push, has been investigated with TDHF theory for one reaction system. The study employed simplified Skyrme interaction and imposed symmetry restriction [41]. Fusion hindrance with modern TDHF simulations has been revealed in several heavy systems [42]. The purpose of the present work is to systematically

[a] e-mail: luguo@ucas.ac.cn

This is an Open Access article distributed under the terms of the Creative Commons Attribution License 2.0, which permits unrestricted use, distribution, and reproduction in any medium, provided the original work is properly cited.

Article available at http://www.epj-conferences.org or http://dx.doi.org/10.1051/epjconf/20123809003

investigate the dynamical fusion threshold with modern TDHF simulation from light to heavy systems, and to answer whether the microscopic TDHF calculation can quantitatively reproduce the extra push predicted with macroscopic model, and to give the criterion for the mass combination of projectile and target above which the extra push is needed, and to indicate the magnitude of extra push energy. In the next Section, we will present Skyrme energy density functional (EDF), static and time-dependent Hartree-Fock theory, nucleus-nucleus interaction potential and numerical details. In Sec. 3, the dynamical fusion threshold in TDHF theory and nucleus-nucleus potential with frozen density approximation will be systematically investigated and compared with available experimental data as well as predictions of macroscopic model. Section 4 is devoted to the summary and conclusions.

2 Theoretical formalism

2.1 Skyrme energy density functional

The zero-range and density-dependent Skyrme force has been widely applied to self-consistent nuclear structure and reaction dynamics calculations owing to its numerical simplicity. The Skyrme energy density functional (EDF)

$$E = \int d^3r H(\rho, \tau, \mathbf{j}, \mathbf{s}, \mathbf{J}), \tag{1}$$

used in the present calculations, is expressed in terms of local densities and currents: density ρ, kinetic density τ, spin density $\mathbf{s}$, current $\mathbf{j}$, and spin-orbit density $\mathbf{J}$. The time-odd terms $\mathbf{s}, \mathbf{j}$ vanish for static calculation of even-even nuclei, whereas they are present for odd-mass nuclei and TDHF. The energy functional H

$$H = H_{\rm kin} + H_{\rm Sk} + H_{\rm C} - H_{\rm c.m.} \tag{2}$$

consists of kinetic energy $H_{\rm kin}$, Skyrme interaction energy $H_{\rm Sk}$, Coulomb energy $H_{\rm C}$ including exchange in Slater approximation, and a correction for the spurious center-of-mass motion $H_{\rm c.m.}$. The pairing correlations are treated in the BCS approximation by using a delta pairing force [43, 44], $V_{pair}(\mathbf{r}, \mathbf{r}') = V_q \delta((\mathbf{r} - \mathbf{r}')$. The pairing strength V_p for protons and V_n for neutrons depend on the mean-field parametrization and are fitted to the pairing gaps in the selected isotopic and isotonic chains [45]. The pairing energy functional is given by

$$H_{\rm pair} = \frac{1}{4} \sum_{q=p,n} V_q \int d^3r \Delta_q^2, \tag{3}$$

with Δ_q the pairing density.

Skyrme energy functional $H_{\rm Sk}$ is expressed as

$$\begin{aligned} H_{\rm Sk} = & \frac{1}{2}t_0(1+\frac{1}{2}x_0)\rho^2 - \frac{1}{2}t_0(\frac{1}{2}+x_0)(\rho_n^2+\rho_p^2) \\ & + \frac{1}{4}(t_1(1+\frac{1}{2}x_1)+t_2(1+\frac{1}{2}x_2))(\rho\tau - \mathbf{j}^2) \\ & - \frac{1}{4}(t_1(\frac{1}{2}+x_1)-t_2(\frac{1}{2}+x_2))(\rho_n\tau_n - \mathbf{j}_n^2 + \rho_p\tau_p - \mathbf{j}_p^2) \\ & - \frac{1}{16}(3t_1(1+\frac{1}{2}x_1)-t_2(1+\frac{1}{2}x_2))\rho\triangle\rho \\ & + \frac{1}{16}(3t_1(\frac{1}{2}+x_1)+t_2(\frac{1}{2}+x_2))(\rho_n\triangle\rho_n + \rho_p\triangle\rho_p) \\ & + \frac{1}{12}t_3(1+\frac{1}{2}x_3)\rho^{2+\alpha} - \frac{1}{12}t_3(\frac{1}{2}+x_3)\rho^{\alpha}(\rho_n^2+\rho_p^2) \\ & - \frac{1}{2}t_4(\rho\nabla\cdot\mathbf{J} + \mathbf{j}\cdot\nabla\times\mathbf{s} + \rho_n\nabla\cdot\mathbf{J}_n + \mathbf{j}_n\cdot\nabla\times\mathbf{s}_n + \\ & + \rho_p\nabla\cdot\mathbf{J}_p + \mathbf{j}_p\cdot\nabla\times\mathbf{s}_p), \end{aligned} \tag{4}$$

with the parameters $t_0, t_1, t_2, t_3, t_4, x_0, x_1, x_2, x_3, \alpha$. The minimum set of time-odd terms to assure Galilei invariance was included. The various parameterizations of Skyrme force are available with different emphasis of nuclear structure properties. We have chosen the SLy6 parametrization [46] in the present calculations, which is widely used and provides a reliable description of nuclear structure and reaction dynamics.

2.2 Static and dynamic EDF

The variation of energy density functional with respect to single-particle wave functions yields the mean-field equation

$$[\hat{h}, \hat{\rho}] = 0 \quad \text{with} \quad \hat{h} = \frac{\partial E}{\partial \hat{\rho}}, \tag{5}$$

which states the simultaneous diagonalization of mean-field Hamiltonian and one-body density. Variation with respect to the occupation amplitudes gives the associated BCS pairing equations. The nuclear ground state wave functions are obtained by solving the coupled HF-BCS equations.

The nuclear large amplitude collective motion has been investigated with TDHF theory. The dynamical evolution of many-body system, denoted by TDHF equation

$$i\hbar\frac{d\hat{\rho}}{dt} = [\hat{h}, \hat{\rho}], \tag{6}$$

is expressed by the time evolution of one-body density. Here the many-body wave functions have been approximated as the independent particle states at any time.

The main advantage of TDHF is that it treats static properties and nuclear dynamics in a unified theoretical framework and the same EDF. Another important advantage of TDHF is that the dynamical effects, e.g., all types of coupling between collective motion and internal excitations, are incorporated automatically. In coupled channel calculations one has to include various excitation modes explicitly according to physical intuition. Last advantage is that there is no free parameters in the description of nuclear dynamics. All the parameters in TDHF theory are from Skyrme functional, which are fitted with nuclear static properties. However TDHF theory include only one-body dissipation and expectation values of one-body observables. The tunneling effect of many-body wave functions has not been taken into account.

2.3 Nucleus-nucleus potential from EDF

A good estimation of the interaction potential between the colliding nuclei can be obtained with EDF using the frozen density (FD) approximation, where the densities of projectile and target are assumed to remain constant and equal

to their respective ground state densities ρ_p and ρ_T. The nucleus-nucleus interaction potential

$$V_{\rm FD}(R) = E[\hat{\rho}_{P+T}](R) - E[\hat{\rho}_P] - E[\hat{\rho}_T] \qquad (7)$$

is expressed in terms of the energy functional E. In FD-EDF method, the functional used in the calculation of nucleus-nucleus potential is same as the Skyrme functional in static and dynamic Hartree-Fock calculations. Note that the Pauli effect was not taken into account in the FD approximation. Around the Coulomb barrier, since the overlap of two densities is small, the fusion barrier with FD-EDF method has been consider to be good approximation.

2.4 Numerical details

The static HF-BCS equations were solved with the damped gradient iteration method [47,48]. We take the variance of the mean-field Hamiltonian, which is required to become smaller than 10^{-4} MeV, as the criterion for convergence. The static HF-BCS wave functions, which give a good nuclear binding energies and deformations, will serve as the initial state in dynamical evolution.

The static and time-dependent Hartree-Fock equations are solved on a cartesian three-dimensional coordinate space. No symmetry restriction has been imposed in the calculation. The spatial derivatives are calculated using the fast Fourier transform and periodic boundary conditions are employed, except for the Coulomb potential, which is calculated with boundary conditions at infinity. The time stepping employs a sixth-order Taylor expansion of the time evolution operator $U(t, t + \Delta t) = \exp[-i\hat{h}(t + \Delta t/2)\Delta t/\hbar]$, with the mean fields at the half step estimated by a third-order expansion using the mean field at time t. The coordinate-space grid consists of $32 \times 24 \times 24$ points for light systems and $48 \times 32 \times 32$ for heavy systems with grid spacing of 1 fm and a time step of 0.2 fm/c. These numerical parameters provide stable and accurate calculations in the sense that good conservation of particle number and total energy has been achieved during the dynamic evolution.

3 Results and discussions

To investigate extra push dynamics in a fully microscopic scenario, one has to compare the lowest bombarding energy, required to achieve fusion for the collision system with fusion barrier. The fusion barrier is the point with maximum potential in the nucleus-nucleus interaction potential. The potential is obtained with the FD-EDF method using the same energy density functional as TDHF, as illustrated in subsection 2.3. Taking ^{64}Ni+^{208}Pb as an example, the nucleus-nucleus interaction potential is shown in the upper panel of figure 1. The fusion barrier $V_{\rm B}$ is 240.02 MeV and locates at a relative distance R_B 13 fm. The lower panel is the time evolution of relative distance between collision parners with different center of mass energy in TDHF calculations. It is seen that the lowest bombarding energy for fusion, denoted as $E_{\rm lf}$ is 262 MeV. Note that the definition of fusion is that a compound system is formed for a minimum duration of 1200 fm/c. The energy difference between low-energy fusion threshold $E_{\rm lf}$ and fusion barrier $V_{\rm B}$ is the additional extra push energy required for

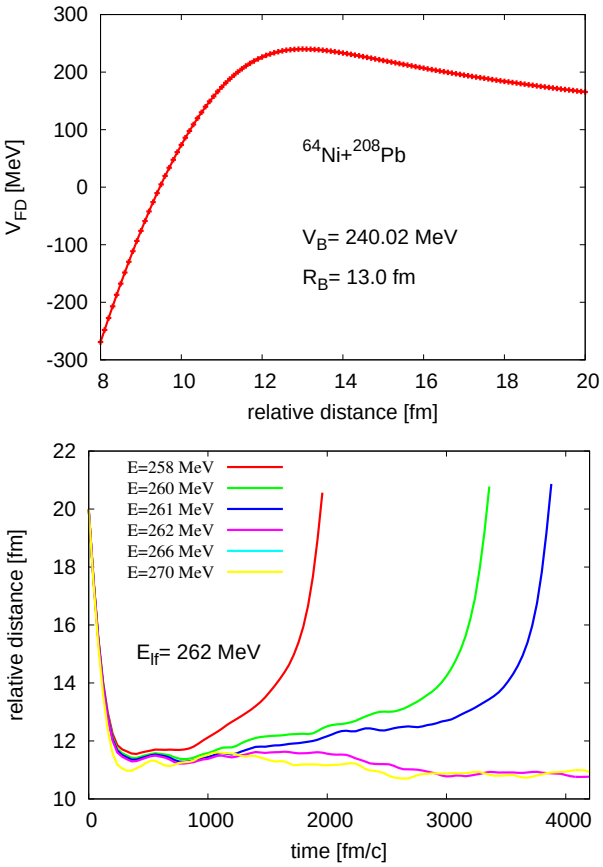

Fig. 1. Nucleus-nucleus interaction potential with FD-EDF method for reaction system ^{64}Ni+^{208}Pb (upper panel); and the time evolution of relative distance in TDHF simulation with different bombarding energy (lower panel).

fusion. In the present example ^{64}Ni+^{208}Pb, extra push energy of at least 22 MeV over fusion barrier is required to make the system fused.

With the same procedure described above, we systematically calculated the fusion barrier and low-energy fusion threshold for the reaction systems of all the combinations among the double magic spherical nuclei ^{16}O, ^{40}Ca, ^{48}Ca, ^{90}Zr, ^{100}Sn, ^{132}Sn, and ^{208}Pb. Additional three systems ^{48}Ca +^{238} U, ^{96}Zr +^{132} Zr, and ^{70}Zn +^{208} Pb, leading to the synthesis of superheavy elements, have also been investigated. In figure 2 the horizontal axis is the effective fissility $(Z^2/A)_{\rm eff} \equiv 4Z_1Z_2/A_1^{1/3}A_2^{1/3}(A_1^{1/3} + A_2^{1/3})$ defined same as in Ref. [36], where Z_1, Z_2, A_1, and A_2 are the proton and atomic mass numbers of the collision partners. The energy difference between TDHF low-energy fusion threshold $E_{\rm lf}^{\rm TDHF}$, fusion barrier with FD-EDF method $V_{\rm B}^{\rm FD}$ and available experimental fusion barrier $V_{\rm B}^{\rm exp}$ are shown in upper panel of figure 2 for all the reaction systems we considered. The extra push energy, denoted as $E_{\rm lf}^{\rm TDHF} - V_{\rm B}^{\rm FD}$ is shown in blue line. Red and green lines represent the deviation of TDHF fusion threshold and FD fusion barrier from the available experiments. As expected, the deviation of TDHF fusion threshold (red line) from experiments is systematically smaller than that of fusion barrier with FD-EDF method (green line). Table 1 lists TDHF fusion threshold $E_{\rm lf}^{\rm TDHF}$, fusion barrier with FD-EDF method $V_{\rm B}^{\rm FD}$ and the experimental fusion barrier $V_{\rm B}^{\rm exp}$, as well as the position of fusion barrier with FD-EDF method $R_{\rm B}^{\rm FD}$

and experiments R_B^{exp}. The microscopic TDHF results are systematically in better agreement with the experiments.

For light systems with effective fissility smaller than 33, TDHF fusion threshold is smaller than fusion barrier with FD-EDF method. Starting from the effective fissility larger than 33, the TDHF fusion threshold becomes larger than FD fusion barrier, indicating the need of extra push. This prediction on the onset of extra push is consistent with Swiatecki's macroscopic model [36]. However, the extra push energy in a fully microscopic TDHF calculation does not monotonic increasing as a function of effective fissility, as seen from the staggering of blue line. For example, the extra push energy of the reaction ^{96}Zr +^{132} Sn with effective fissility $(Z^2/A)_{\rm eff}$ = 35.48 is about 11.35 MeV, while its neighboring reaction system ^{90}Zr+^{90}Zr with $(Z^2/A)_{\rm eff}$ = 35.56 has extra push energy of -1.7 MeV. Since the collision dynamics is affected by many factors, e.g., nuclear structure and dynamical effects in the time evolution, the extra push energy will not simply depend on the mass combination.

The lower panel in figure 2 shows the prediction of extra push in Swiatecki's macroscopic model [36] in purple line and our TDHF result same as the blue line in upper panel. The extra push energy in macroscopic model is much larger than our microscopic results especially for heavier systems. For example, TDHF and macroscopic extra push energy of four labelled reaction systems ^{48}Ca +^{238} U, ^{96}Zr +^{132} Zr, ^{70}Zn +^{208} Pb, and ^{100}Sn +^{132} Sn are 0.87 MeV and 0.048 MeV , 11.35 MeV and 6.43 MeV, 19.18 MeV and 49 MeV, 25.75 MeV and 116.84 MeV. This is not strange owing to the following facts. The macroscopic model did not take into account many important dynamical effects. Moreover the parameters in macroscopic extra push formula is fitted with several experimental fusion cross section with the heaviest system $(Z^2/A)_{\rm eff}$ = 39.044 [36]. The way to fit the parameters may restrict the reliability of the extrapolation of macroscopic extra push formula to heavier system than $(Z^2/A)_{\rm eff}$ = 39.044. Recently, the experimental evidence [38–40] also indicates that the extra push energy, needed in the formation of heavy and superheavy systems, is smaller than the prediction with Swiatecki's macroscopic model [36].

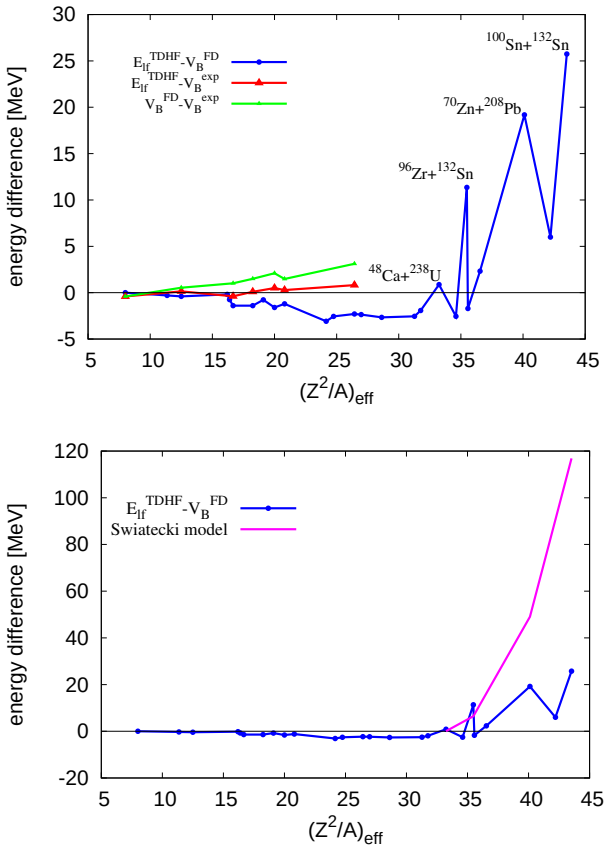

Fig. 2. Energy difference between TDHF low-energy fusion threshold and fusion barrier with FD-EDF method (blue line), TDHF fusion threshold and available experimental data (red line), and fusion barrier with FD-EDF method and available experiments (green line) as a function of effective fissility (upper panel); energy difference between TDHF low-energy fusion threshold and fusion barrier with FD-EDF method in blue line, and the prediction of extra push formula in Swiatecki's macroscoic model in purple line (lower panel).

Table 1. TDHF low-energy fusion threshold E_{lf}^{TDHF} (in MeV), fusion barrier with FD-EDF method V_B^{FD} (in MeV), the experimental fusion barrier V_B^{exp} (in MeV), and their position of fusion barrier R_B^{FD} (in fm) and R_B^{exp} (in fm).

reaction	E_{lf}^{TDHF}	V_B^{FD}	V_B^{exp}	R_B^{FD}	R_B^{exp}
^{16}O+^{16}O	10.2	10.2	10.61	8.4	7.91
^{16}O+^{40}Ca	23.2	23.6	23.06	9.2	9.21
^{40}Ca+^{40}Ca	53.3	54.9	52.8	9.8	—
^{40}Ca+^{48}Ca	52.1	53.5	52.0	10.1	9.99
^{48}Ca+^{48}Ca	51.1	52.5	51.49	10.3	10.16
^{16}O+^{208}Pb	74.8	76.0	74.52	11.7	11.31
^{40}Ca+^{90}Zr	97.7	100.0	96.88	10.8	10.53

4 Summary

TDHF fusion threshold and fusion barrier with FD-EDF method have been systematically investigated for the reaction systems of all the combinations among the double magic spherical nuclei ^{16}O, ^{40}Ca, ^{48}Ca, ^{90}Zr, ^{100}Sn, ^{132}Sn, and ^{208}Pb, as well as additional three systems ^{48}Ca +^{238} U, ^{96}Zr +^{132} Zr, and ^{70}Zn +^{208} Pb leading to the synthesis of superheavy elements. TDHF fusion threshold is in better agreement with the experimental fusion barrier. We find that the onset of extra push lies at effective fissility 33, which is consistent with the prediction of macroscopic model. However the extra push energy in our microscopic calculations is systematically smaller than the prediction with macroscopic model especially for heavier system. The way to fit the parameters and the important dynamical effects neglected in macroscopic model might be responsible for the different results between TDHF calculation and macroscopic model. Experimental evidence also indicates that the extra push energy is smaller than the predictions with macroscopic model.

Acknowledgments

This work was supported in part by the Natural Science Foundation of China (Grants No. 11175252) and the President Fund of GUCAS. The calculations were performed

by using the RIKEN Integrated Cluster of Clusters (RICC) facility.

References

1. J. Blocki, J. Randrup, W.J. Swiatecki, and C.F. Tsang, Ann. Phys. (NY) **105**, 427 (1977)
2. H.J. Krappe, J.R. Nix, and A.J. Sierk, Phys. Rev. C **20**, 992 (1979)
3. G. Satchler and W. Love, Phys. Rep. **55**, 183 (1979)
4. C. H. Dasso, S. Landowne, and A. Winther, Nucl. Phys. A **405**, 381 (1983)
5. W. Reisdorf, J. Phys. G: Nucl. Part. Phys. **20**, 1297 (1994)
6. A.B. Balantekin and N. Takigawa, Rev. Mod. Phys. **70**, 77 (1998)
7. W.D. Myers and W.J. Swiatecki, Phys. Rev. C **62**, 044610 (2000)
8. K. Hagino, N. Rowley, and A.T. Kruppa, Comput. Phys. Commun. **123**, 143 (1999)
9. J.O. Newton, R.D. Butt, M. Dasgupta, D.J. Hinde, I.I Gontchar, C.R.Morton, and K. Hagino, Phys.Rev.C **70**, 024605 (2004)
10. P.A.M. Dirac, Proc. Cambridge Phil. Soc. **26**, 376 (1930)
11. P. Bonche, S.E. Koonin, and J.W. Negele, Phys. Rev. C **13**, 1226 (1976)
12. K.T.R. Davies, H.T. Feldmeier, H. Flocard, and M.S. Weiss, Phys. Rev. C **18**, 2631 (1978)
13. H. Flocard, S.E. Koonin, and M.S. Weiss, Phys. Rev. C **17**, 1682 (1978)
14. P. Bonche, B. Grammaticos, and S. Koonin, Phys. Rev. C **17**, 1700 (1978)
15. W. Negele, Rev. Mod. Phys. **54**, 913 (1982)
16. P.-G. Reinhard, A.S. Umar, K.T.R. Davies, M.R. Strayer, and S.-J. Lee, Phys. Rev. C **37**, 1026 (1988)
17. C. Simenel and P. Chomaz, Phys. Rev. C **68**, 024302 (2003)
18. C. Simenel, P. Chomaz, and G. de France, Phys. Rev. Lett. **93**, 102701 (2004)
19. T. Nakatsukasa and K. Yabana, Phys. Rev. C **71**, 024301 (2005)
20. A.S. Umar and V.E.Oberacker, Phys. Rev. C **71**, 034314 (2005)
21. J.A. Maruhn, P.-G. Reinhard, P.D. Stevenson, J.R. Stone, and M.R. Strayer, Phys. Rev. C **71**, 064328 (2005)
22. J.A. Maruhn, P.-G.Reinhard, P.D. Stevenson, and M.R. Strayer, Phys. Rev. C **74**, 027601 (2006)
23. A.S. Umar and V.E. Oberacker, Phys. Rev. C **74**, 024606 (2006)
24. P.-G. Reinhard, L. Guo, and J.A. Maruhn, Eur. Phys. J. A **32**, 19 (2007)
25. L. Guo, J.A. Maruhn, and P.-G. Reinhard, Phys. Rev. C **76**, 014601 (2007)
26. L. Guo, J.A. Maruhn, P.-G. Reinhard, and Y. Hashimoto, Phys. Rev. C **77**, 041301(R) (2008)
27. K. Washiyama, and D. Lacroix, Phys. Rev. C **78**, 024610 (2008)
28. K. Washiyama, S. Ayik, and D. Lacroix, Phys. Rev. C **80**, 031602(R) (2009)
29. A.S. Umar, V.E. Oberacker, Phys. Rev. C **77**, 064605 (2008)
30. A.S. Umar, V.E. Oberacker, J.A. Maruhn, and P. -G. Reinhard, Phys. Rev. C **80**, 041601 (2009)
31. C. Simenel, Phys. Rev. Lett. **105**, 192701 (2010)
32. Y. Iwata, T. Otsuka, J.A. Maruhn, and N. Itagaki, Phys. Rev. Lett. **104**, 252501 (2010)
33. C. Simenel, Phys. Rev. Lett. **106**, 112502 (2011)
34. R. Keser, A.S. Umar, and V.E. Oberacker, Phys. Rev. C **85**, 044606 (2012)
35. S. Fracasso, E.B. Suckling, and P.D. Stevenson, Phys. Rev. C **86**, 044303 (2012)
36. W.J. Swiatecki, Nucl. Phys. A **376**, 275 (1982)
37. H. Gaggeler, Z. Phys. A **316**, 291 (1984)
38. W. Reisdorf and M. Schadel, Z. Phys. A. **343**, 47 (1992)
39. S. Hofmann, Rep. Prog. Phys. **61**, 639 (1998)
40. G. Giardina, S. Hofmann, A.I. Muminov, and A.K. Nasirov, Eur. Phys. J. A **8**, 205 (2000)
41. J.A. Maruhn, K.T.R. Davies, and M.R. Strayer, Phys. Rev. C **31**, 1289 (1985)
42. C. Simenel and B. Avez, arXiv:0904.2653v1.
43. F. Tondeur, Phys. Lett. B **123**, 139 (1983)
44. S.J. Krieger, P. Bonche, H. Flocard, P. Quentin, and M.S. Weiss, Nucl. Phys. A **517**, 275 (1990)
45. P. Fleischer, P. Klupfel, P.-G. Reinhard, and J.A. Maruhn, Phys. Rev. C **70**, 054321 (2004)
46. E. Chabanat, E.P. Bonche, P. Haensel, J. Meyer, and R. Schaeffer, Nucl. Phys. A **635**, 231 (1998)
47. V. Blum, G. Lauritsch, J.A. Maruhn, and P.-G. Reinhard, J. Comput. Phys. **100**, 364 (1992)
48. P.-G. Reinhard and R.Y. Cusson, Nucl. Phys. A **378**, 418 (1982)